ACS APPLIED ELECTRONIC MATERIALS

Article

Cite This: ACS Appl. Electron. Mater. 2019, 1, 1890−1898

pubs.acs.org/acsaelm

Molecular Approach To Enhance Thermal Conductivity in Electrically Conductive Adhesives

Li-Ting Tseng, Ren-Huai Jhang, Jing-Qian Ho, and Chun-Hu Chen*

Department of Chemistry, National Sun Yat-sen University, Kaohsiung, Taiwan 80424

Supporting Information

ABSTRACT: Significant heat generation in modern high-speed electronic devices requires elevated thermal conductivity of electrically conductive adhesives (ECAs), but the gap between discrete filler materials significantly interrupts the pathway of heat transport. In this work, we demonstrated the 587% enhancement of thermal conductivity by adding a silver−organic complex (i.e., silver 2-ethylhexanoate) in an epoxy-based ECA with the optimal value of 4.7 W/mK at a low curing temperature of 180 °C. After the postannealing at 200 °C, the thermal conductivity can be further enhanced to 6.2 W/mK with high stability. In the presence of the silver−organic complex, the optimal die shear strength can be increased to 179% (38.06 MPa) compared to that of the blank samples. The silver−organic complex is capable of molecule-scale blending and forming ultrafine Ag particles (13−47 nm) well-distributed in the epoxy matrix, enabling gap-filling and bulky network sintering to achieve thermal conductivity enhancement.

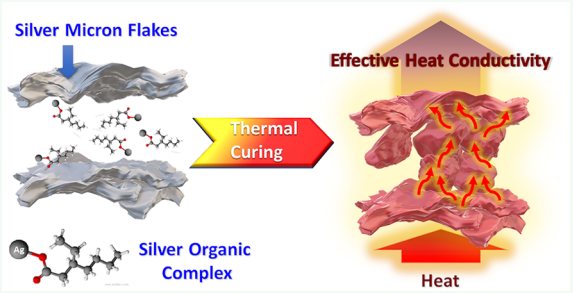

KEYWORDS: *thermal conductivity, silver 2-ethylhexanoate, adhesive, silver, paste*

1. INTRODUCTION

Conventional solders like Sn/Pb are now deemed to be highly hazardous to the environment and unsuitable for applications requiring high spatial resolution. Electrically conductive adhesives (ECAs) comprised of various polymers and conductive fillers are widely used in the electronics industry for the advantages of easy processing, low soldering temperatures, and the capability of microscale patterning.[1−3] To date, ECAs are used in a versatile way for fabrication in microelectronics, solar cells, and flexible devices.[4−14] Epoxy-based adhesives have better adhesion, greater chemical stability, and lower shrinkage compared to other resin systems.[3,9,15] They are widely combined with Ag fillers as commercial products for industrial usage. The characteristic low soldering temperatures and high flexibility of ECAs lead toward their emerging impact on printed electronics (e.g., radio frequency identification, RFID).[4−7]

The rising challenge for ECAs is the dissipation of excessive heat generated by modern high-performance devices, such as high-speed internet antennae, high-power light emitting diodes (LEDs), and electronic packaging procedures.[16−18] Thermal interface materials (TIMs) are frequently used to fill the gaps between an integrated circuit (IC) and a heat sink for an efficient heat transfer.[19] To achieve high thermal conductivity, micron-flake fillers such as metals (e.g., Cu, Ag, Ni, Al, etc.)[20−22] and carbon/nitride materials (e.g., graphene, carbon nanotube, BN, etc.)[17,23−26] have been reported. Obtaining elevated thermal conductivity in ECAs is greatly hindered by discontinuous contact between micron-flake fillers because of interruption by epoxy resins.[27−29] Great attempts to fill out these gaps has been focused on establishing continuous pathways or channels to transport heat. However, the large density mismatch between the fillers and epoxy matrix causes ineffective gap filling due to an inhomogeneous distribution/segregation of filler particles. Furthermore, the issues on inhomogeneity are also challenging for the industry because of the lack of long-term storage and processing reliability. Despite the relatively small density mismatch by using carbon fillers (e.g., carbon nanotube/graphene sheets), their intrinsically strong tangling and interstacking behaviors result in the significant increase of viscosity, which is problematic for industrial usage.[30]

In silver-based ECAs, dimensional modification of Ag fillers, such as changes in particle sizes and aspect ratios, were frequently conducted to improve thermal/electrical conductivities. Chiang's group showed that enlarged micron-sized Ag flakes (up to tens of microns) can improve thermal conductivity by 40%.[12] Silver nanosized powders were proposed to fill out the gaps of fillers and give more continuous channels.[31−33] Usage of one-dimensional Ag nanowires (high aspect ratios) increased thermal conductivity due to their interconnected thermal conductive channels.[14,34] However, similar to one-dimensional carbon fillers, the huge exposed surface area of Ag nanowires and nanosized powders could interact with the resin matrix, resulting in a severe increase of viscosity.[31,35] As long as metallic Ag fillers are used,

Received: June 24, 2019
Accepted: August 26, 2019
Published: August 26, 2019

DOI: 10.1021/acsaelm.9b00401
ACS Appl. Electron. Mater. 2019, 1, 1890−1898

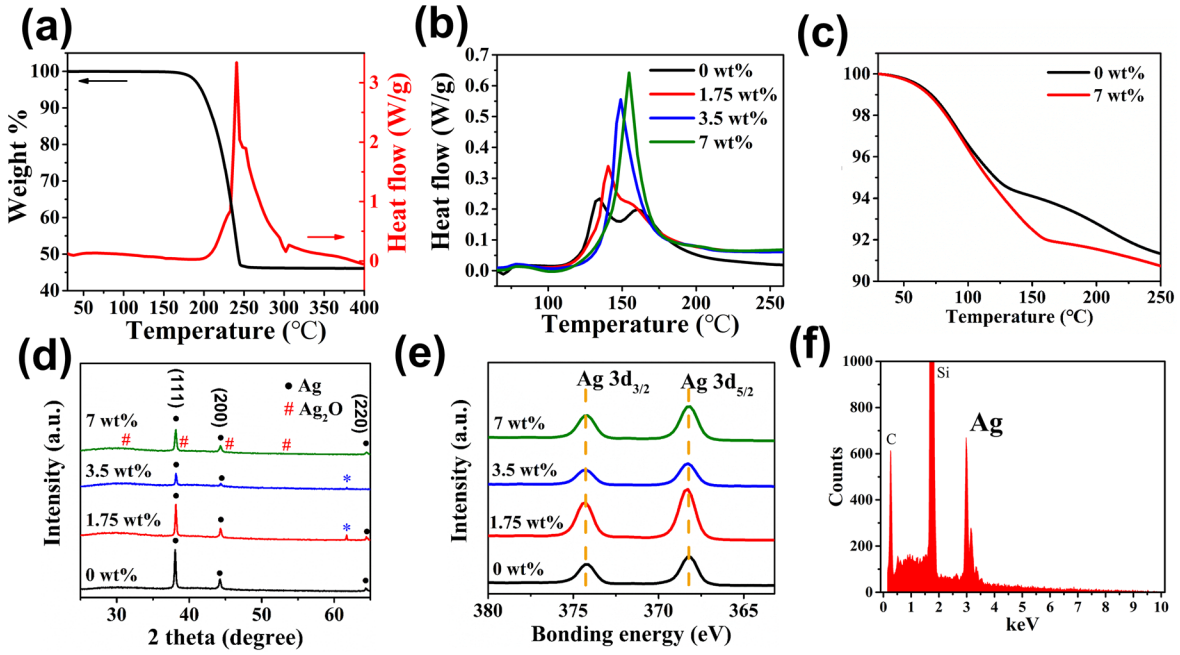

Figure 1. Thermal behavior of the silver−organic complex (AgEH) and characterization of the as-yielded particles. (a) The DSC (red) and TGA (black) curves of AgEH that decomposes at 240 °C; (b) the DSC curves of ECA samples containing different amounts of AgEH showing the exothermic peaks at 135−155 °C but no peaks corresponding to AgEH decomposition at 240 °C. (c) The TGA profiles showing different weight losses between 0 and 7 wt % AgEH samples starting at 130 °C, close to the temperature range of the exothermic peaks in (b). (d) The XRD patterns show metallic silver in all the ECA samples without oxidized phases; the absent Ag_2O phase is indicated by the pound (#) label. The star label (*) indicates the background signals. (e) XPS characterization results of all the ECA samples also show metallic silver only. (f) The typical EDXS elemental analysis of the AgEH-yielded ultrafine nanoparticles in the ECA after thermal curing.

density mismatch issues may always remain unsolved. As a result, complicated surface modification and/or preparation procedures for Ag filler materials are required to improve their homogeneity in ECAs.[36,37] For example, the surface modification of Ag fillers using fatty acids has been extensively conducted to improve their dispersive capability in polymer environments.[31] However, the insulating effects of the fatty acids inhibit the electrical conductivity of the ECA.[38]

To address these challenges, we utilized a silver−organic complex (SOC) as a molecular approach aiming to accomplish highly continuous, thermally conductive channels in Ag ECAs. Before thermal curing, the molecular form of the SOC can be facilely processed and evenly distributed within the epoxy without issues on density mismatch. Upon thermal curing, SOC is anticipated to generate Ag nanoparticles on-site along the matrix, which serves to fill up the discontinuous gaps with high probability. The previous report used a series of SOCs in solvents to reduce electrical resistivity;[39] Vaseem et al. have pioneered in formulating particle-free silver inks aiming toward printable electronics on soft substrates,[40] but the role of using SOCs as an ECA additive in thermal conductivity improvement has not yet been explored. Potential gap-filling functionality using the molecular approach still remains elusive.

In this work, we demonstrated the significant thermal conductivity enhancement by adding silver 2-ethylhexanoate (AgEH) as the SOC into epoxy-based Ag ECAs. After curing at 180 °C, AgEH transformed into ultrafine Ag nanoparticles (13−46 nm) and effectively filled out the interparticle space to enhance thermal conductivity by more than 580% compared to that of the blank samples (AgEH-free). The shear strength of the SOC-added ECAs is shown to be greatly improved as well. The cross section studies showed that sintering of the Ag micron fillers yields a highly continuous Ag network to facilitate heat transport.

2. EXPERIMENTAL SECTION

2.1. Synthesis of Silver 2-Ethylhexanoate. Aqueous sodium hydroxide (4 M) was first mixed with 2-ethylhexanoic acid (3.07 g) to form a clear colorless solution, followed by the addition of silver nitrate (4 M). The white precipitate of silver 2-ethylhexanoate (AgEH) was formed immediately. After filtration, the white precipitate was washed by ethanol (100 mL) under vigorous stirring for 10 min and then cleaned by acetone (100 mL) for another 10 min of stirring. The as-treated products were then dried completely under vacuum for 3 h. The as-obtained AgEH was characterized by matching with commercially available standards (Strem Chemical Inc.) using IR spectroscopy (Spectrum Two, PerkinElmer) and an X-ray diffraction (XRD) database (Figure S-1).

2.2. Preparation of ECAs. Specific quantities of epoxy resin (BCHC 200, bisphenol A epoxy resin), curing agents (I17−60, imidazole series), and silane coupling agents (MHS-003) were mixed first. Fillers of both of the Ag microflakes (AFTL-M5, diameter: 3−5 μm) and dendrite-like Ag aggregates (ASTL-SN500, diameter: 0.1−0.3 μm) (Figure S-2) were added to the mixture homogeneously using a three-roller mill at room temperature to yield paste-like ECA samples. All the chemicals and Ag materials were supplied by the Ample Electronic Technology Company without further purification before use. The total mass percent of the Ag fillers was 66% in the blank ECA, which does not contain any SOC. The added amounts of AgEH (i.e., 1.75, 3.5, and 7 wt %) were counted as extra additives with respect to the mass of the blank ECA. Thus, the blank sample can also be considered as 0 wt % AgEH-added ECA.

2.3. Characterization. The thermal decomposition properties of ECA samples were measured through thermogravimetric analysis (TGA) using a TGA 4000 (PerkinElmer Co.) and differential scanning calorimetry (DSC) using a DSC 1 (Mettler Toledo Inc.) in both air and nitrogen atmospheres. The temperature range of the TGA measurement was 30−400 °C with a heating rate of 10 °C·

DOI: 10.1021/acsaelm.9b00401
ACS Appl. Electron. Mater. 2019, 1, 1890−1898

min^{-1}. The bulk resistance (R) of the ECAs was measured by a digital ohmmeter AX-1142N (Adex Aile Co.). Meanwhile, the width and thickness of each specimen were measured using a surface roughness tester (Surfcom 1400D, Accretech Co.) to accurately determine the bulk resistivity ρ of each sample using the following equation: $\rho = Rtw/l$, where the l, t, and w are the length, thickness, and width of the sample, respectively. The thermal conductivity measurements of the ECAs were conducted at room temperature by a Thermal Constants Analyzer (TPS 2500 S, Hot Disk, standard mode). The paste samples were placed in a vacuum oven at room temperatures for 2 h, and a revolution−rotation motion mixer was used to completely remove the gas bubbles. The pastes were then squeezed into a round-disk mold and then cured at 180 °C. The products were polished by sandpaper. The dimensions of the disks for thermal conductivity measurement were 2.5 cm in diameter by 1 mm in thickness. The stability tests of thermal conductivity were conducted by annealing the samples at 200 °C for every 2 h, followed by naturally cooling each sample down to room temperature for thermal conductivity measurement. For the thin-layer sampling, each ECA sample was spin-coated on a wafer (3000 rpm for 30 s), cured at a specific temperature, and then subjected to an FEI Inspect F50d and Zeiss Supra 55 Gemini Scanning Electron Microscope (SEM) to determine the morphology of each material. Elemental compositions of the samples were analyzed by energy dispersive X-ray spectroscopy (EDXS) under SEM. The particle size distribution of each sample was processed using ImageJ software by randomly sampling at least 100 particles (spots) from the acquired SEM images. X-ray photoelectron spectroscopy (XPS) measurements were obtained on a PHI 5000 VersaProbe with a monochromatic Al Kα X-ray as the excitation source (ULVAC-PHI, Inc.). X-ray diffraction (XRD) data were acquired using a Bruker D2 Phaser (Bruker Co.) diffractometer with a Cu Kα X-ray source. The samples for XPS and XRD analyses were prepared following the procedure identical to the SEM sample preparation. For adhesion test, Si chips (1 mm × 1 mm) were attached on copper substrates using the as-prepared ECA samples via a dispensing robot (OKTEK Co.) and then cured at 180 °C in N_2 for 1 h. Shear tests of these glued samples were carried out using a bond tester (series 4000, test module: DS100, Nordson DAGE Co.). The rheology was measured with 20 mm parallel plate geometry at 25 °C with 1.0 Hz by a hybrid rheometer (Discovery HR-2, TA Instruments). For the bulk resistance measurement, each ECA sample was poured into a stripe stencil with a width of 1 mm and then leveled to form ordered ECA stripes (length: 1−2 cm, width: 1 mm, height: 15−20 μm). These molded ECA stripes were then cured at different temperatures (160, 180, 210, 240 °C) for 1 h to produce samples for conductivity measurement. For thermal conductivity measurement, the ECAs were degassed in a vacuum oven at room temperature for 2 h and then placed into a planetary centrifugal mixer. Subsequently, each mixture was cast within an aluminum mold to produce round-shape plate samples that were 4 cm in diameter by 0.5 cm thick.

3. RESULTS

3.1. Thermal Decomposition of Silver−Organic Complex. The thermal properties of AgEH and the AgEH-added ECAs are shown in Figure 1. The TGA/DSC results of AgEH complex in air reveal an exothermic peak corresponding to the thermal decomposition at 240 °C. In the blank ECA samples (0 wt % AgEH), a small exothermic peak starting around 120 °C is presumably attributed to the exothermic curing of the epoxy according to the control sample, which contains the epoxy and curing agents only (Figure S-3). As AgEH is added, the DSC profiles (Figure 1b) show stronger and sharper exothermic signals at 135−155 °C. Note that the signal pertaining to the decomposition of AgEH at 240 °C was absent among all the AgEH ECA samples shown in Figure 1b. This may be due to the interactions between the epoxy matrix and organic content of AgEH, which improve the dissociation of AgEH. This also correlates to the TGA results (Figure 1c) showing that the 2% loss in mass due to the organic content in AgEH occurs at around 130−160 °C for the 7 wt % AgEH ECAs. The systematic peak shift to lower temperatures as more epoxy is present in the mixture might be due to the less unconfined decomposition of AgEH within the epoxy network. Also, the 2% mass loss observed in TGA (Figure 1c) is lower than its theoretical values of 3.73% if all organic components of AgEH are decomposed completely. This suggests that some organic components of AgEH are still partly trapped within the epoxy matrix.

3.2. Ultrafine Ag Particle Formation and Cross Section Study. To investigate the resultants of AgEH after the thermal decomposition in the epoxy, we conducted a thin-layer sampling by first spin-coating ECA on Si wafers, followed by baking at 180 °C for 60 min. In the blank ECA samples (Figure 2a), the SEM images show the two typical Ag fillers,

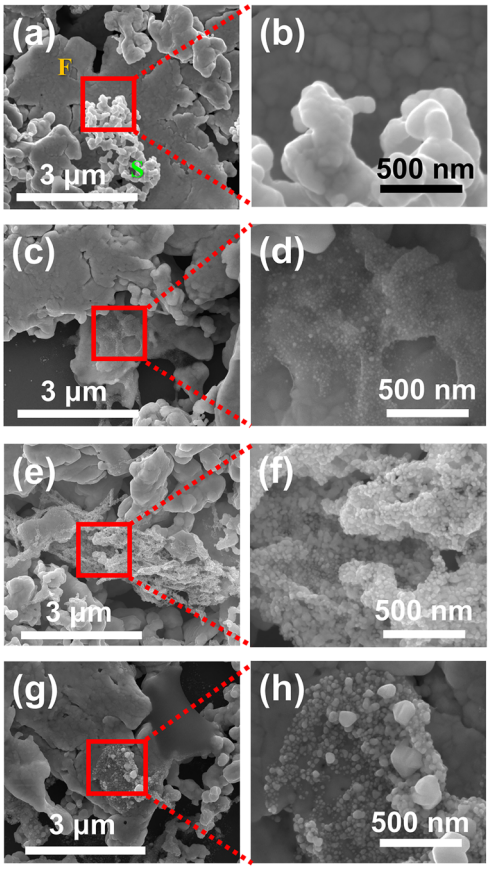

Figure 2. SEM images of the ECAs containing varied amounts of AgEH. All the samples were prepared by thin-layer sampling followed by baking at 180 °C. (a,b) 0 wt %, (c,d) 1.75 wt %, (e,f) 3.5 wt %, and (g,h) 7 wt %. The red squares indicate the corresponding high-magnification images. The labels of F (Ag microflakes) and S (submicron Ag aggregates) in (a) demonstrate the two types of Ag fillers in all the ECA samples. The AgEH-yielded ultrafine Ag particles are clearly formed within the epoxy resin.

the micron flakes (the orange "F" labels) and submicron dendrite-like aggregates (the green "S" labels), which are chosen to be contained within the ECA samples for this work. Ag micron flakes are commonly used as fillers mainly responsible for acquiring electrical conductivity sufficient for device operation, whereas the dendrite-like aggregates were

DOI: 10.1021/acsaelm.9b00401
ACS Appl. Electron. Mater. 2019, 1, 1890−1898

used intentionally to mimic the strategy of improving electrical and/or thermal conductivity with Ag nanopowders.[6,12,31−33]

The magnified images in Figure 2b show the aggregation of Ag whose particle diameter is around 100−300 nm. After the addition of 1.75 wt % AgEH, the SEM images (Figure 2c,d) reveal the presence of ultrafine, aggregate-free nanoparticles with an average diameter of 13.3 ± 2.9 nm (Figure S-4), apart from the two Ag fillers (Figure 2a). These ultrafine Ag nanoparticles, which are drastically different from the two Ag fillers, are well-distributed along the resin matrix (Figures 2d and S-5).

By increasing the AgEH addition to 3.5 wt %, the diameters of the particles (15.9 ± 4.4 nm, Figure 2e,f) were increasing with size-distribution behaviors similar to the 1.75 wt % samples (Figure S-4). For the sample with the highest AgEH content (7 wt %), the diameter of the particles significantly increased (46.5 ± 30.8 nm, Figure 2g,h). It also contains much larger size variation compared to the 1.75 and 3.5 wt % cases (Figure S-4), suggesting the local concentration inhomogeneity of AgEH when the adding amount increases to a certain level.

Material characterization of the AgEH-yielded ultrafine particles was carried out using XRD, XPS, and EDXS. The XRD patterns of the Ag fillers in the blank samples correspond to a metallic Ag phase (Figure 1d); the XPS data (Figure 1e) show the signals of Ag $3d_{5/2}$ and $3d_{3/2}$ at 368.3 and 374.3 eV, respectively, verifying the presence of metallic Ag only without the oxide forms.[41] All the AgEH-added samples show that both the XRD and XPS results identical to the blank samples, indicating that these ultrafine particles yielded by AgEH thermal decomposition are only metallic Ag, rather than silver oxide. The EDXS results (Figures 1f and S-6) confirm that these ultrafine particles consist of Ag. These results confirm that metallic Ag nanoparticles can be produced within the epoxy matrix at 180 °C among all the AgEH samples. The molecular-scale dispersion of AgEH results in the well-suspended ultrafine Ag particles in the epoxy for the higher probability of gap filling.

We further conducted a cross section study where the cured ECA samples immobilize Si chips onto the Cu surface. As shown in Figure 3a, the SEM images of the blank ECA show random-sized gaps due to discontinuous packing of the Ag fillers. By adding 1.75 wt % AgEH, certain regions of the discontinuous fillers merge into more continuous, bulkier Ag "chunks". Nevertheless, these chunks were not yet vertically connecting the top Si chips and the bottom Cu surface. The cross section of 3.5 wt % samples also exhibits the generation of merged Ag chunks (Figure 3c), whereas the coalescence of Ag fillers in the 7 wt % samples is highly pronounced, which results in a vertically continuous pathway connecting the Si chip and Cu substrates (Figure 3d). SOC addition is shown to be highly effective for filling out the gap between the Ag fillers. Aside from the physical gap filling, the presence of AgEH seems to also assist in the sintering of the Ag fillers to yield continuous networks, which is desired to effectively facilitate heat transport.

3.3. Thermal and Electrical Conductivity. The thermal conductivities and densities of ECAs cured at 180 °C as a function of AgEH weight percent are shown together in Figure 4a. The increase in thermal conductivity can be observed by increasing the amounts of AgEH. In the blank sample, the thermal conductivity is 0.8 W/mK, which is comparable to the usual epoxy ECAs reported in the literature.[42,43] The thermal conductivity values for ECAs with 1.75, 3.5, and 7 wt % of

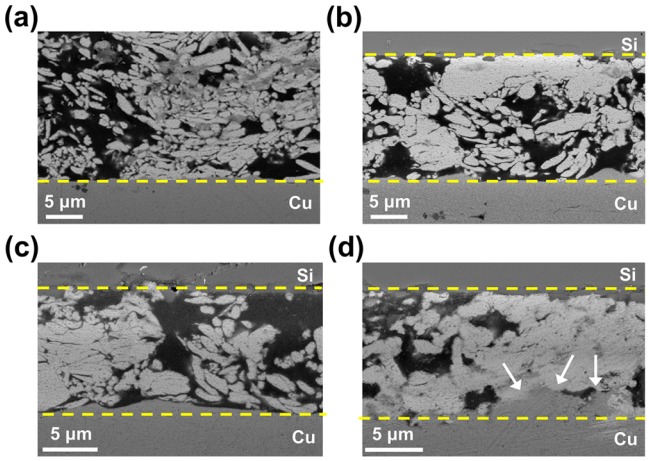

Figure 3. Cross section SEM images of ECAs with varied amounts of AgEH after the 180 °C curing. The ECA was applied to immobilize Si chips (top layer of the images) on Cu substrates (bottom layer of the images). (a) 0 wt %, (b) 1.75 wt %, (c) 3.5 wt %, and (d) 7 wt %. The yellow dash lines are the boundary between the ECA and Si chips and Cu substrates. The addition of AgEH not only filled out the gap between discrete fillers of Ag microflakes but also sintered these fillers to establish a more continuous Ag network to enhance the thermal conductivity. The white arrows in (d) indicate the Cu/Ag contact due to intrusion of Cu.

AgEH are 1.9, 2.2, and 4.7 W/mK, respectively. The comparable thermal conductivity values between the 1.75 and 3.5 wt % samples are actually consistent with their similarity in cross section SEM images (Figure 3). The optimized addition of 7 wt % AgEH achieves a 587% thermal conductivity with respect to the blank samples and is also higher than the thermal conductivities of the 1.75 and 3.5 wt % samples. Such a strong enhancement can be attributed to the successful formation of vertically continuous Ag networks, according to the cross section SEM results. On the other hand, we also compared the efficacy of using nanosized Ag powders with the molecular approach. The equivalent Ag mass in 7 wt % AgEH was substituted by the dendrite-like Ag aggregates for ECA sample preparation, which exhibited the thermal conductivity of 1.68 W/mK. This thermal conductivity value corresponds to just 84, 76, and 36% with respect to the samples loaded with 1.75, 3.5, and 7 wt % of AgEHs, respectively. Thus, the effective construction of a continuous Ag network by a molecular approach indeed shows a more crucial impact on thermal conductivity improvement.

In addition, the stability tests of the thermal conductivity with the 7 wt % AgEH showed increased values up to 6.2 (W/mK) after the first 2 h thermal annealing period (Figure 4b). Such the increase of thermal conductivity is most likely due to the improved contacts among the continuous Ag networks, as reported in the literature.[44] After another 2 h of aging, this enhanced value remains unchanged, showing the high stability of the thermal conductivity of the epoxy-based adhesives.

Figure 4b shows the changes of the electrical resistivity of AgEH-added ECA samples as a function of curing temperatures. The higher curing temperatures generally lowered the resistivity. An increase of the curing temperature enables higher degrees of the ECA volume shrinking, which leads to a higher probability of interparticle contact between the Ag fillers.[45,46] In the presence of 1.75 wt % AgEH, the resistivity of the obtained ECA is generally smaller than that of the blank

DOI: 10.1021/acsaelm.9b00401
ACS Appl. Electron. Mater. 2019, 1, 1890−1898

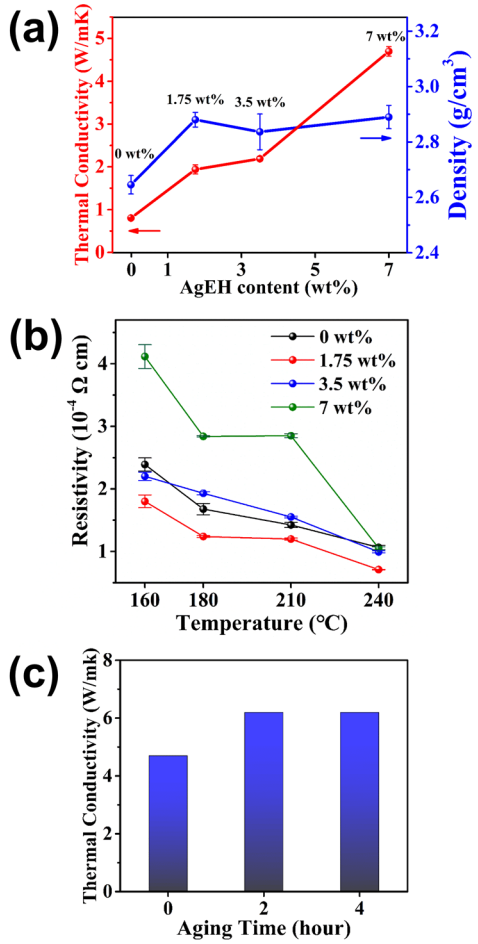

Figure 4. Thermal conductivity and electrical resistivity of the ECA samples. (a) The dependence of the thermal conductivity and density on the varied amounts of AgEH in ECAs cured at 180 °C. (b) The dependence of the electrical resistivity on the curing temperatures. (c) The stability test of the thermal conductivity of 7 wt % AgEH ECAs aged at 200 °C.

samples over the entire temperature range, exhibiting the lowest value of 7.5×10^{-5} Ω·cm at 240 °C. Meanwhile, the addition of 3.5 and 7 wt % AgEH reverses the trend by increasing the resistivity. At 180 °C, the increasing order of resistivity among samples is 1.75 wt % (1.2×10^{-4} Ω·cm) < 0 wt % (1.7×10^{-4} Ω·cm) < 3.5 wt % (1.9×10^{-4} Ω·cm) < 7 wt % (2.8×10^{-4} Ω·cm), which despite the variations within a small magnitude, can all meet the conductivity requirements for applications such as light emitting diodes (LEDs).[12]

The density of the blank ECA was 2.65 g/cm^3 (Figure 4a). Meanwhile, the densities of the AgEH-added samples are 2.88 g/cm^3 (1.75 wt %), 2.84 g/cm^3 (3.5 wt %), and 2.89 g/cm^3 (7 wt %). The results presented a significant density change between the blank and AgEH-added samples, whereas a much smaller variation was noted among the 1.75 to 7 wt % samples. Using the blank ECA as reference, the estimated total weight of the samples should be as follows: blank ECA (100%) < 1.75 wt % AgEH (100 + 1.75%) < 3.5 wt % AgEH (100 + 3.5%) < 7 wt % AgEH (100 + 7%). Under the assumption of identical volume shrinking and weight loss during resin curing, the estimated densities of cured ECAs should be following the same order above. The density of the 1.75 wt % sample is most likely higher than the anticipated values by the trend. The overshrinking of the epoxy volume usually results in the density fluctuation, according to the literature.[46,47] Because elevated density increases the contact between micron Ag flakes and thus electrical conductivity,[32,48] the overshooting density of 1.75 wt % ECA may rationalize the lowest resistivity observed in Figure 4b.

3.4. Rheological Properties and Shear Adhesion. We measured the viscosity changes dependent on the AgEH contents of ECAs before curing (Figure 5a). The viscosity profiles as a function of shear rates exhibit a typical shear thinning behavior, in which the ones containing more AgEH result in greater viscosity values. The viscosity value of the paste containing 7 wt % AgEH is 3050 mPa·s at a shear rate of 500 s^{-1}, which is 3.7 times higher than that with 1.75 wt % AgEH (827.4 mPa·s). This systematic increase in viscosity of the AgEH pastes suggests the presence of a molecular-scale interaction among AgEH, Ag particles, and epoxy matrix.[31,49] A relatively large viscosity increase at a low shear rate suggests that a high yield stress is required to break the strengthened network. This observation manifests the advantage of achieving a well-dispersed SOC within the epoxy matrix as opposed to blending solid Ag particles. Our study also indicates that the viscosities of pastes can be modulated by solvents to address the processing concern.

Figure 5b shows the die shear strength comparisons of AgEH-added ECAs cured at 180 °C. The AgEH-added ECAs show shear strength values of 31.62, 31.20, and 38.06 MPa by adding 1.75, 3.5, and 7 wt % of AgEH, respectively. The optimal shear strength of the 7 wt % sample is 179% with respect to the blank ECAs (21.23 MPa). As shown in the cross section SEM images (Figure 3), the Cu substrates tend to intrude into the ECA region to form an intimate contact with the Ag fillers (see particularly the region indicated by the arrows in Figure 3d). Such an additional contact due to the AgEH addition may be attributed to an increase of the shear

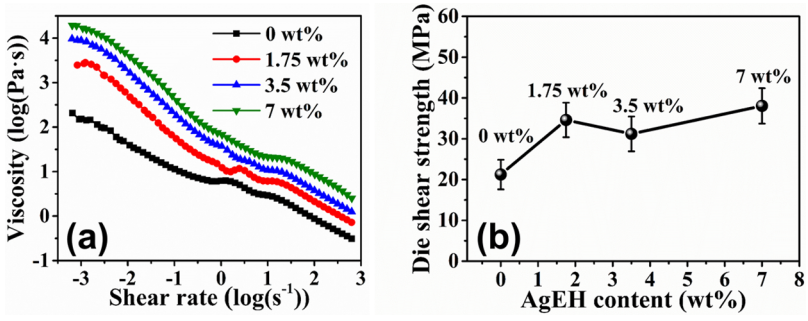

Figure 5. Mechanical behaviors of the ECAs with different amounts of AgEH. (a) The profiles of viscosity and (b) shear strength comparison.

DOI: 10.1021/acsaelm.9b00401
ACS Appl. Electron. Mater. 2019, 1, 1890−1898

Scheme 1. Schematic Comparison of Thermal Conductivity Enhancement between Adding the Silver−Organic Complex and Ag Nanosized Powders in ECAs[a]

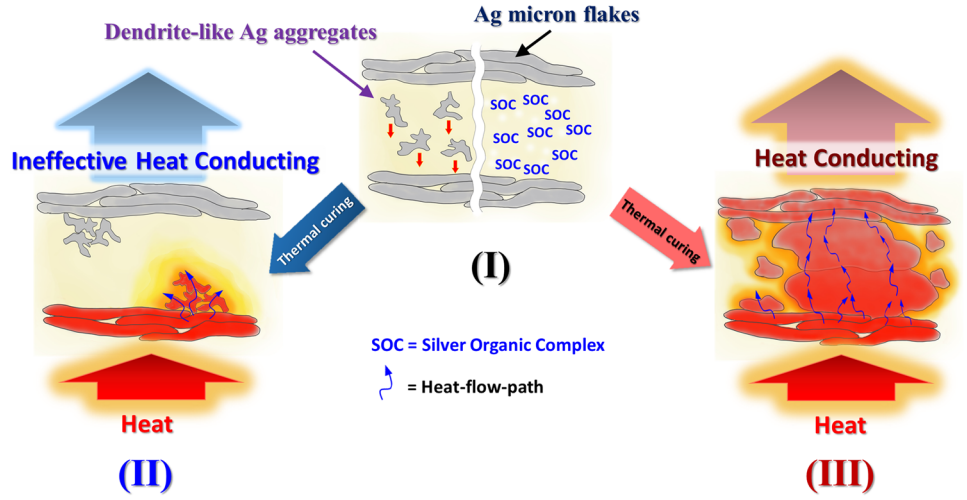

[a](I) Before thermal curing, the SOC can be homogeneously blended in the epoxy resin with high compatibility (on the right), but the dendrite-like Ag aggregates (on the left) tend to sink down gradually in contact with the flakes because of a large density mismatch with the resin. (II) After thermal curing, the Ag aggregates are not able to conduct heat effectively due to the insufficient gap-filling capability. (III) In contrast, the thermally decomposed SOC results in the well-dispersed Ag ultrafine particles that effectively fill out the gap between the micron flakes and thus significantly enhances the heat transport. Note that the realistic scales between objects are not consistent with each other for the clear presentation of the concept.

strength. Usually, the decreased percentages of epoxy in ECAs lead to the weaker adhesion. Meaning, the increase of Ag content would help in gaining higher electrical and thermal conductivities at the expense of the reduced shear strength.[50,51] Thus, it is difficult to keep adhesion intact while adding Ag powders for the purpose of improved thermal/electrical conductivity in ECAs. Our results demonstrate that, by adopting the molecular strategy of using an SOC, the improved adhesion and thermal conductivity can be achieved simultaneously without compromising the performance of either. The adhesion strength of AgEH-added ECAs is shown to be superior or comparable to those of reported systems with varying filler contents, a mixed polymer/epoxy matrix, and different substrate−chip couples.[50,52]

4. DISCUSSION

The thermal conductivity enhancement is highly associated with the formation of ultrafine Ag nanoparticles through AgEH. Formation of metallic Ag particles requires reduction of Ag(I) ions, which usually occurs by adding reducing agents and/or thermal treatments.[53−56] The organic anion of AgEH (i.e., $CH_3(CH_2)_3CH(C_2H_5)COO^-$) contains a carboxylic group that could thermally decompose to generate CO_2 as an oxidation product, coupling with the reduction of Ag(I) into metallic silver.[56−58] The chemical equation can be expressed as suggested in the literature[59,60]

$$2RCOOAg(s) \rightarrow 2Ag(s) + 2CO_2(g) + R_2(s) \quad (1)$$

To effectively accomplish the gap-filling capability, it is necessary to have the precursor occupying the space between the fillers. Upon thermal curing, decomposition of the precursor followed by the on-site growth of Ag ultrafine particles could potentially close up the gap. The selective distribution of AgEH-yielded particles in the epoxy region indicates the ideal situation in that the silver−organic complex blends well within the epoxy matrix. The growth of silver ultrafine particles starts from the nucleation of Ag atoms following eq 1. The initial nucleating clusters of Ag should shortly exist with much smaller diameters than those of the particles (Figure 2) that already reached thermodynamic equilibrium after the completed curing process. These kinetic-dependent Ag clusters should possess much lowered melting points that allow sintering with other clusters or fillers during the thermal curing process.[61−63] With the high loading level of 7 wt %, a locally inhomogeneous distribution of AgEH might result in a wide particle size distribution suitable to fill up the gap with various dimensions. As silver materials are mainly responsible for heat transport in the ECAs, the highly continuous Ag networks could therefore be crucial for such purposes. In contrast, the density mismatch issues could still tend to sink down the dendrite-like aggregates, leading to an ineffective formation of continuous Ag networks. This potential mechanism of molecular-enhanced thermal conductivity has been summarized in Scheme 1.

According to the cross section SEM images, the CO_2 release in eq 1 does not clearly yield bubbles and/or porosities in the cured AgEH ECAs, including the blank samples (Figure 3). Thus, there is no direct evidence showing that CO_2 "bubbles" are actually present in the cured ECAs, although the CO_2 release after AgEH thermal decomposition has been both proven in the literature[50−52] and also observed in our temperature-programmed decomposition-mass spectrometry (TPD-MS) experiments (see Figure S-7). Before the detailed investigation, the absence of bubble-form CO_2 may be plausibly attributed to the low content of AgEH in the samples, and/or some electron donor groups (e.g., amine groups) in the adhesives may interact with CO_2 to yield other forms of compounds, inhibiting bubble formation. In fact, both the thermal conductivity and mechanical behaviors of the AgEH-added ECA are improved with the increased AgEH content, suggesting that CO_2 generation may not significantly impact the ECA performance in this study.

DOI: 10.1021/acsaelm.9b00401
ACS Appl. Electron. Mater. 2019, 1, 1890−1898

5. CONCLUSION

In this work, we demonstrated the enhanced thermal conductivity and shear strength of epoxy ECAs through the addition of AgEH as a silver−organic complex. In contrast to adding Ag nanosized powders, a molecular approach yielding well-suspended ultrafine Ag particles in a resin environment holds the key to effectively realize continuous Ag networks. As the thermal conductivity values are proportional to the AgEH contents, there might be more room for further optimization. Further studies of understanding the decreased decomposition temperatures of a silver−organic complex in an ECA environment are critical for the rational design of low curing temperature products. Exploration of diverse silver−organic complexes capable of increasing the thermal conductivity of ECAs is actively under pursuit.

■ ASSOCIATED CONTENT

Supporting Information

The Supporting Information is available free of charge on the ACS Publications website at DOI: 10.1021/acsaelm.9b00401.

Characterization of the silver−organic complex (XRD and IR); SEM images of Ag fillers and ultrafine particles; DSC, EDS, and TPD-MS data of the ECA products; particle size-distribution study (PDF)

■ AUTHOR INFORMATION

Corresponding Author

*E-mail: chunhu.chen@mail.nsysu.edu.tw.

ORCID

Ren-Huai Jhang: 0000-0002-8439-5446

Chun-Hu Chen: 0000-0002-3512-6880

Author Contributions

The manuscript was written through contributions of all authors. All authors have given approval to the final version of the manuscript.

Notes

The authors declare no competing financial interest.

■ ACKNOWLEDGMENTS

We acknowledge the financial support from the Ministry of Science and Technology, Taiwan under grant 107-2622-M-110-001-CC2. We also thank Joey Andrew A. Valinton for the help on cover artwork production.

■ REFERENCES

(1) Jiang, H.; Moon, K.-s.; Li, Y.; Wong, C. P. Surface Functionalized Silver Nanoparticles for Ultrahigh Conductive Polymer Composites. *Chem. Mater.* **2006**, *18*, 2969−2973.

(2) Tan, F.; Qiao, X.; Chen, J.; Wang, H. Effects of Coupling Agents on the Properties of Epoxy-based Electrically Conductive Adhesives. *Int. J. Adhes. Adhes.* **2006**, *26*, 406−413.

(3) Chen, S.; Liu, K.; Luo, Y.; Jia, D.; Gao, H.; Hu, G.; Liu, L. In Situ Preparation and Sintering of Silver Nanoparticles for Low-cost and Highly Reliable Conductive Adhesive. *Int. J. Adhes. Adhes.* **2013**, *45*, 138−143.

(4) Ren, H. M.; Guo, Y.; Huang, S. Y.; Zhang, K.; Yuen, M. M.; Fu, X. Z.; Yu, S.; Sun, R.; Wong, C. P. One-Step Preparation of Silver Hexagonal Microsheets as Electrically Conductive Adhesive Fillers for Printed Electronics. *ACS Appl. Mater. Interfaces* **2015**, *7*, 13685−13692.

(5) Yang, R.; Wang, Y.; Wu, D.; Deng, Y.; Luo, Y.; Cui, X.; Wang, X.; Shu, Z.; Yang, C. Low-Temperature Fusible Silver Micro/Nanodendrites-Based Electrically Conductive Composites for Next-Generation Printed Fuse-Links. *ACS Nano* **2017**, *11*, 7710−7718.

(6) Ji, Y. H.; Liu, Y.; Huang, G. W.; Shen, X. J.; Xiao, H. M.; Fu, S. Y. Ternary Ag/epoxy Adhesive with Excellent Overall Performance. *ACS Appl. Mater. Interfaces* **2015**, *7*, 8041−8052.

(7) Shen, Y.; Chen, Z.; Zhou, T.; Feng, W.; Liu, Y. Green Preparation of Flaky Silver Powders with Nano-thickness Towards Electrically Conductive Adhesives Through A Nanofilm Transition Method. *J. Mater. Chem. C* **2016**, *4*, 254−258.

(8) Cauchy, X.; Klemberg-Sapieha, J. E.; Therriault, D. Synthesis of Highly Conductive, Uniformly Silver-Coated Carbon Nanofibers by Electroless Deposition. *ACS Appl. Mater. Interfaces* **2017**, *9*, 29010−29020.

(9) Lim, H. S.; Kim, S.-N.; Lim, J. A.; Park, S.-D. Low Temperature-cured Electrically Conductive Pastes for Interconnection on Electronic Devices. *J. Mater. Chem.* **2012**, *22*, 20529−20534.

(10) Shin, D. Y.; Seo, J. Y.; Kang, M. G.; Song, H. E. Contact Resistivity Decrease at A Metal/semiconductor Interface by A Solid-to-liquid Phase Transitional Metallo-organic Silver. *ACS Appl. Mater. Interfaces* **2014**, *6*, 15933−15941.

(11) Wang, Z.; Liang, X.; Zhao, T.; Hu, Y.; Zhu, P.; Sun, R. Facile Synthesis of Monodisperse Silver Nanoparticles for Screen Printing Conductive Inks. *J. Mater. Sci.: Mater. Electron.* **2017**, *28*, 16939−16947.

(12) Chiang, T. H.; Lin, Y.-C.; Chen, Y.-F.; Chen, E.-Y. Effect of Anhydride Curing Agents, Imidazoles, and Silver Particle Sizes on The Electrical Resistivity and Thermal Conductivity in the Silver Adhesives of LED Devices. *J. Appl. Polym. Sci.* **2016**, *133*, 43587.

(13) Cui, H.-W.; Fan, Q.; Li, D.-S. Surface Functionalization of Micro Silver Flakes and Their Application in Electrically Conductive Adhesives for Electronic Package. *Int. J. Adhes. Adhes.* **2014**, *48*, 177−182.

(14) Zhao, T.; Zhang, C.; Du, Z.; Li, H.; Zou, W. Functionalization of AgNWs with Amino Groups and Their Application in An Epoxy Matrix for Antistatic and Thermally Conductive Nanocomposites. *RSC Adv.* **2015**, *5*, 91516−91523.

(15) Gu, H.; Ma, C.; Gu, J.; Guo, J.; Yan, X.; Huang, J.; Zhang, Q.; Guo, Z. An Overview of Multifunctional Epoxy Nanocomposites. *J. Mater. Chem. C* **2016**, *4*, 5890−5906.

(16) Fu, Y.-X.; He, Z.-X.; Mo, D.-C.; Lu, S.-S. Thermal Conductivity Enhancement with Different Fillers for Epoxy Resin Adhesives. *Appl. Therm. Eng.* **2014**, *66*, 493−498.

(17) Shtein, M.; Nadiv, R.; Buzaglo, M.; Kahil, K.; Regev, O. Thermally Conductive Graphene-Polymer Composites: Size, Percolation, and Synergy Effects. *Chem. Mater.* **2015**, *27*, 2100−2106.

(18) Liu, S.; Zhao, B.; Jiang, L.; Zhu, Y.-W.; Fu, X.-Z.; Sun, R.; Xu, J.-B.; Wong, C.-P. Core−shell Cu@rGO Hybrids Filled in Epoxy Composites with High Thermal Conduction. *J. Mater. Chem. C* **2018**, *6*, 257−265.

(19) Zulkarnain, M.; Fadzil, M. A.; Mariatti, M.; Azid, I. A. Effects of Silver Microparticles and Nanoparticles on Thermal and Electrical Characteristics of Electrically Conductive Adhesives. *J. Electron. Mater.* **2017**, *46*, 6727−6735.

(20) Halaciuga, I.; Njagi, J. I.; Redford, K.; Goia, D. V. Deposition of Continuous Nickel Shells on Polymer Microspheres. *J. Colloid Interface Sci.* **2012**, *383*, 215−221.

(21) Qi, S.; Litchfield, R.; Hutt, D. A.; Vaidhyanathan, B.; Liu, C.; Webb, P.; Ebbens, S. Copper Conductive Adhesives for Printed Circuit Interconnects. *IEEE 62nd Electronic Components and Technology Conference* **2012**, 1651−1655.

(22) Yang, C.; Xie, Y.-T.; Yuen, M. M.-F.; Xu, B.; Gao, B.; Xiong, X.; Wong, C. P. Silver Surface Iodination for Enhancing the Conductivity of Conductive Composites. *Adv. Funct. Mater.* **2010**, *20*, 2580−2587.

(23) Yang, X.; He, W.; Wang, S.; Zhou, G.; Tang, Y. Preparation and Properties of a Novel Electrically Conductive Adhesive Using A Composite of Silver Nanorods, Silver Nanoparticles, and Modified Epoxy Resin. *J. Mater. Sci.: Mater. Electron.* **2012**, *23*, 108−114.

(24) Li, Q.; Guo, Y.; Li, W.; Qiu, S.; Zhu, C.; Wei, X.; Chen, M.; Liu, C.; Liao, S.; Gong, Y.; Mishra, A. K.; Liu, L. Ultrahigh Thermal

Conductivity of Assembled Aligned Multilayer Graphene/Epoxy Composite. *Chem. Mater.* **2014**, *26*, 4459−4465.
(25) Liu, Z.; Chen, Y.; Li, Y.; Dai, W.; Yan, Q.; Alam, F. E.; Du, S.; Wang, Z.; Nishimura, K.; Jiang, N.; Lin, C.-T.; Yu, J. Graphene Foam-embedded Epoxy Composites with Significant Thermal Conductivity Enhancement. *Nanoscale* **2019**.
(26) Alam, F. E.; Dai, W.; Yang, M.; Du, S.; Li, X.; Yu, J.; Jiang, N.; Lin, C.-T. In Situ Formation of A Cellular Graphene Framework in Thermoplastic Composites Leading to Superior Thermal Conductivity. *J. Mater. Chem. A* **2017**, *5*, 6164−6169.
(27) Dai, W.; Lv, L.; Lu, J.; Hou, H.; Yan, Q.; Alam, F. E.; Li, Y.; Zeng, X.; Yu, J.; Wei, Q.; Xu, X.; Wu, J.; Jiang, N.; Du, S.; Sun, R.; Xu, J.; Wong, C.-P.; Lin, C.-T. A Paper-Like Inorganic Thermal Interface Material Composed of Hierarchically Structured Graphene/Silicon Carbide Nanorods. *ACS Nano* **2019**, *13*, 1547−1554.
(28) Lv, L.; Dai, W.; Li, A.; Lin, C.-T. Graphene-Based Thermal Interface Materials: An Application-Oriented Perspective on Architecture Design. *Polymers* **2018**, *10*, 1201.
(29) Hou, H.; Dai, W.; Yan, Q.; Lv, L.; Alam, F. E.; Yang, M.; Yao, Y.; Zeng, X.; Xu, J.-B.; Yu, J.; Jiang, N.; Lin, C.-T. Graphene Size-dependent Modulation of Graphene Frameworks Contributing to the Superior Thermal Conductivity of Epoxy Composites. *J. Mater. Chem. A* **2018**, *6*, 12091−12097.
(30) Lan, W.-J.; Chen, C.-H. Hybridization of Graphene in 3D Complex Nanovoids: Synergistic Nanocomposites for Electrocatalytic Reduction of Hydrogen Peroxide. *Electrochim. Acta* **2015**, *180*, 1014−1022.
(31) Zhang, R.; Lin, W.; Moon, K. S.; Wong, C. P. Fast Preparation of Printable Highly Conductive Polymer Nanocomposites by Thermal Decomposition of Silver Carboxylate and Sintering of Silver Nanoparticles. *ACS Appl. Mater. Interfaces* **2010**, *2*, 2637−2645.
(32) Lee, H.-H.; Chou, K.-S.; Shih, Z.-W. Effect of Nano-sized Silver Particles on the Resistivity of Polymeric Conductive Adhesives. *Int. J. Adhes. Adhes.* **2005**, *25*, 437−441.
(33) Jiang, H.; Moon, K.-s.; Li, Y.; Wong, C. P. Surface Functionalized Silver Nanoparticles for Ultrahigh Conductive Polymer Composites. *Chem. Mater.* **2006**, *18*, 2969−2973.
(34) Yu, Y.-H.; Ma, C.-C. M.; Teng, C.-C.; Huang, Y.-L.; Tien, H.-W.; Lee, S.-H.; Wang, I. Enhanced Thermal and Mechanical Properties of Epoxy Composites Filled with Silver Nanowires and Nanoparticles. *J. Taiwan Inst. Chem. Eng.* **2013**, *44*, 654−659.
(35) Wu, H.; Chiang, S.; Han, W.; Tang, Y.; Kang, F.; Yang, C. Surface Iodination: A Simple and Efficient Protocol to Improve the Isotropically Thermal Conductivity of Silver-epoxy Pastes. *Compos. Sci. Technol.* **2014**, *99*, 109−116.
(36) Gu, J.; Liang, C.; Dang, J.; Dong, W.; Zhang, Q. Ideal Dielectric Thermally Conductive Bismaleimide Nanocomposites Filled with Polyhedral Oligomeric Silsesquioxane Functionalized Nanosized Boron Nitride. *RSC Adv.* **2016**, *6*, 35809−35814.
(37) Huang, X.; Iizuka, T.; Jiang, P.; Ohki, Y.; Tanaka, T. Role of Interface on the Thermal Conductivity of Highly Filled Dielectric Epoxy/AlN Composites. *J. Phys. Chem. C* **2012**, *116*, 13629−13639.
(38) Li, C.; Li, Q.; Long, X.; Li, T.; Zhao, J.; Zhang, K.; E, S.; Zhang, J.; Li, Z.; Yao, Y. In Situ Generation of Photosensitive Silver Halide for Improving the Conductivity of Electrically Conductive Adhesives. *ACS Appl. Mater. Interfaces* **2017**, *9*, 29047−29054.
(39) Lu, C.-A.; Lin, P.; Lin, H.-C.; Wang, S.-F. Characterization of the Low-Curing-Temperature Silver Paste with Silver 2-Ethylhexanoate Addition. *Jpn. J. Appl. Phys.* **2007**, *46*, 251−255.
(40) Vaseem, M.; McKerricher, G.; Shamim, A. Robust Design of a Particle-Free Silver-Organo-Complex Ink with High Conductivity and Inkjet Stability for Flexible Electronics. *ACS Appl. Mater. Interfaces* **2016**, *8*, 177−186.
(41) Moulder, J. F. *Handbook of X-ray Photoelectron Spectroscopy: A Reference Book of Standard Spectra for Identification and Interpretation of XPS Data*; Chastain, J., Ed.; Physical Electronics Division, Perkin-Elmer Corporation, 1992.
(42) Suh, D.; Moon, C. M.; Kim, D.; Baik, S. Ultrahigh Thermal Conductivity of Interface Materials by Silver-Functionalized Carbon Nanotube Phonon Conduits. *Adv. Mater.* **2016**, *28*, 7220−7227.
(43) Pashayi, K.; Fard, H. R.; Lai, F.; Iruvanti, S.; Plawsky, J.; Borca-Tasciuc, T. High Thermal Conductivity Epoxy-silver Composites Based on Self-constructed Nanostructured Metallic Networks. *J. Appl. Phys.* **2012**, *111*, 104310.
(44) Inoue, M.; Muta, H.; Maekawa, T.; Yamanaka, S.; Suganuma, K. Temperature Dependence of Electrical and Thermal Conductivities of an Epoxy-Based Isotropic Conductive Adhesive. *J. Electron. Mater.* **2008**, *37*, 462−468.
(45) Lin, H.-C.; Lin, P.; Lu, C.-A.; Wang, S.-F. Effects of Silver Oxalate Additions on the Physical Characteristics of Low-temperature-curing MOD Silver Paste for Thick-film Applications. *Microelectron. Eng.* **2009**, *86*, 2316−2319.
(46) Daoqiang, L.; Wong, C. P. Effects of Shrinkage on Conductivity of Isotropic Conductive Adhesives. *International Symposium on Advanced Packaging Materials. Processes, Properties and Interfaces* **1999**, 295−301.
(47) Nawab, Y.; Tardif, X.; Boyard, N.; Sobotka, V.; Casari, P.; Jacquemin, F. Determination and Modelling of the Cure Shrinkage of Epoxy Vinylester Resin and Associated Composites by Considering Thermal Gradients. *Compos. Sci. Technol.* **2012**, *73*, 81−87.
(48) Mach, P.; Radev, R.; Pietrikova, A. Electrically Conductive Adhesive Filled with Mixture ofSilver Nano and Microparticles. *IEEE 2nd Electronics Systemintegration Technology Conference* **2008**, 1141−1146.
(49) Ekere, N. N.; Durairaj, R.; Salam, B. Thixotropy Low Behaviour of Solder and Conductive Adhesive Pastes. *J. Mater. Sci.: Mater. Electron.* **2004**, *15*, 677−683.
(50) Kishi, H.; Tanaka, S.; Nakashima, Y.; Saruwatari, T. Self-assembled Three-dimensional Structure of Epoxy/polyethersulphone/silver Adhesives with Electrical Conductivity. *Polymer* **2016**, *82*, 93−99.
(51) Trinidad, J.; Chen, L.; Lian, A.; Zhao, B. Solvent Presence and Its Impact on the Lap-shear Strength of SDS-decorated Graphene Hybrid Electrically Conductive Adhesives. *Int. J. Adhes. Adhes.* **2017**, *78*, 102−110.
(52) Guan, Y.; Chen, X.; Li, F.; Gao, H. Study on the Curing Process and Shearing Tests of Die Attachment by Ag-epoxy Electrically Conductive Adhesive. *Int. J. Adhes. Adhes.* **2010**, *30*, 80−88.
(53) Smeets, P. J. M.; Cho, K. R.; Kempen, R. G. E.; Sommerdijk, N. A. J. M.; De Yoreo, J. J. Calcium Carbonate Nucleation Driven by Ion Binding in A Biomimetic Matrix Revealed by In Situ Electron Microscopy. *Nat. Mater.* **2015**, *14*, 394−399.
(54) Hill, E. H.; Hanske, C.; Johnson, A.; Yate, L.; Jelitto, H.; Schneider, G. A.; Liz-Marzán, L. M. Metal Nanoparticle Growth within Clay−Polymer Nacre-Inspired Materials for Improved Catalysis and Plasmonic Detection in Complex Biofluids. *Langmuir* **2017**, *33*, 8774−8783.
(55) Yao, Y.; Zeng, X.; Sun, R.; Xu, J.-B.; Wong, C.-P. Highly Thermally Conductive Composite Papers Prepared Based on the Thought of Bioinspired Engineering. *ACS Appl. Mater. Interfaces* **2016**, *8*, 15645−15653.
(56) Liu, J.; Chen, H.; Ji, H.; Li, M. Highly Conductive Cu−Cu Joint Formation by Low-Temperature Sintering of Formic Acid-Treated Cu Nanoparticles. *ACS Appl. Mater. Interfaces* **2016**, *8*, 33289−33298.
(57) Fragalà, M. E.; Malandrino, G.; Puglisi, O.; Benelli, C. Synthesis, X-ray Structure, and Characterization of Ag(hfa)·Tetraglyme [hfa = Hexafluoroacetylacetonate]: A Novel Adduct for the Fabrication of Metallic Silver Based Films via in Situ Self Reduction. *Chem. Mater.* **2000**, *12*, 290−293.
(58) Rill, M. S.; Plet, C.; Thiel, M.; Staude, I.; von Freymann, G.; Linden, S.; Wegener, M. Photonic Metamaterials by Direct Laser Writing and Silver Chemical Vapour Deposition. *Nat. Mater.* **2008**, *7*, 543−546.

DOI: 10.1021/acsaelm.9b00401
ACS Appl. Electron. Mater. 2019, 1, 1890−1898

(59) Nakano, M.; Fujiwara, T.; Koga, N. Thermal Decomposition of Silver Acetate: Physico-Geometrical Kinetic Features and Formation of Silver Nanoparticles. *J. Phys. Chem. C* **2016**, *120*, 8841−8854.
(60) Szczęsny, R.; Szłyk, E. Thermal Decomposition of Some Silver(I) Carboxylates under Nitrogen Atmosphere. *J. Therm. Anal. Calorim.* **2013**, *111*, 1325−1330.
(61) Ide, E.; Angata, S.; Hirose, A.; Kobayashi, K. F. Metal−metal Bonding Process Using Ag Metallo-organic Nanoparticles. *Acta Mater.* **2005**, *53*, 2385−2393.
(62) Yan, J.; Zou, G.; Wu, A.-p.; Ren, J.; Yan, J.; Hu, A.; Zhou, Y. Pressureless Bonding Process Using Ag Nanoparticle Paste for Flexible Electronics Packaging. *Scr. Mater.* **2012**, *66*, 582−585.
(63) Wang, S.; Li, M.; Ji, H.; Wang, C. Rapid Pressureless Low-temperature Sintering of Ag Nanoparticles for High-power Density Electronic Packaging. *Scr. Mater.* **2013**, *69*, 789−792.

DOI: 10.1021/acsaelm.9b00401
ACS Appl. Electron. Mater. 2019, 1, 1890−1898